THE PERFORMANCE ANALYSIS OF WRF ON GHI PREDICTION IN TWO DIFFERENT REGIONS OF TURKEY

Seyda Tilev Tanriover[1] Abdullah Kahraman[1] Erhan Çalışkan[1-2]

Selahattin İncecik[1] Ceyhan Kahya[1] Sema Topçu[1] Bülent Aksoy[3]

[1)] Istanbul Technical University, Department of Meteorological Engineering,

34469 Maslak-Istanbul tanriovers@itu.edu.tr

[2)] io Environmental Solutions R&D Co., 34469 Maslak-Istanbul

[3)]Turkish State Meteorological Service, 06120 Kecioren-Ankara

ABSTRACT

The Performance Analysis of WRF on GHI Prediction in Two Different Regions of Turkey

The aim of this study is to 72 hour forecast of hourly global horizontal irradiation (GHI) using WRF model and to analyze the effect of parameterization on model performance for the two different periods including clear sky and cloudy conditions. Particularly, GHI forecast evaluation was carried out for the periods of August 20-23, 2011 as clear sky condition and May 8-11, 2011 as partly cloudy condition.

Performance of the WRF model using different radiation, microphysics and boundary layer parameterization configurations was verified against ground observations.

Keywords: WRF, GHI, Solar Radiation Prediction

1. Introduction

Globally renewable energy continued to grow strongly. Specifically, solar power generation is growing fast, expanding from marginal levels in 2000 to an estimated 65 TWh in 2012 (44.7% annually) (IEA, 2013). The capacity in solar PV is expanded with a 29-30 GW in 2012. Currently, 23 IEA countries represented 89.5 GW of cumulative PV installation and PV electricity is estimated to have a technical potential of 205 GW by 2020 or about 2% of global electricity demand (IEA, 2011). According to recent Special Report for renewable energies by the IPCC (2011) solar energy technologies harness the energy of solar irradiance to produce electricity using PV and CSP systems. The development in the field of the solar energy it makes the key data for the design and application of solar energy systems.

Turkey ranks among the fastest growing energy markets in the World and is the 17th largest economy in the world, and total electricity demand in 2010 was 211 TWh (Ozer et al., 2013). Turkeys electrical consumption reached to 229.3 billion kWh in 2011. But the PV contribution to electricity consumption in Turkey did not exceed 0.01% while 2.79% in Spain, 5.57% in Germany and 5.75% in Italy (IEA, 2013).

Suri et al., (2007) noticed that the highest potential for solar electricity generation is in the Mediterranean region including southern parts of Turkey. There are several studies indicating the usage of solar energy resources with a promising prospect for the future as an alternative to conventional energy in Turkey. (Incecik et al., 2012; Alta et al., 2010, Bulut and Büyükalaca, 2007; Bakırcı, 2009). Because, Turkey (36-42 0N) has been recognized as a region with abundant availability of solar irradiation in Mediterranean belt. Specifically, South Eastern Anatolia of Turkey (SEA) is highly favorable geographical location for the utilization of solar energy similar to Spain and Portugal. This region has the most significant region of country with 1460 kWh-m2/year total solar radiation and 2993 h sunshine duration while the country has an average 1311 kWh/m2-year and 2640 hr sunshine duration (EIEI, 2013). On the other hand, one of the least solar potential region of the Turkey is Marmara region which is located at the northwest of the country. This region has 1168 kWh/m2- year and 2409 hr sunshine duration.

Generally, global solar radiation data can be provided from routine ground-based measurements. However as solar power plants are built and integrated into the electricity grid, it is important to know how much solar energy is produced in the next 2-3 days for the entire management of total power production from different sources decision making in the energy market and helpful for the grid operators in order to better accommodate the variable generation of electricity in scheduling, and regulation of power. But, the global solar irradiation is highly variable and is mainly dependent on cloudiness, relative humidity and aerosols (Ohtake et al., 2012). Thus, accurate solar forecasts over short time horizons are required for solar power planning and production and therefore forecast of solar irradiation is critical (Inman et al., 2013). An efficient use of the fluctuating energy output requires reliable forecast.

Numerical Weather Prediction (NWP) models have been proved to be powerful tools for solar radiation forecasting (Lara-Fanego et al., 2012; Lara-Fanego et al., 2011;Lorenz et al., 2009). NWP models predict Global Horizontal Irradiance (GHI) resolving physical processes and using radiation transfer models (Morcretie et al., 2007). Early model evaluations for estimating GHI was based on MM5 mesoscale model (Grell et al., 1998; Heinemann et al., 2006; Zamora et al., 2003 and Zamora et al., 2005). These studies were carried out in some locations in the USA (Zamora et al., 2003 and Zamora et al., 2005) and for some locations in Europe such as Germany, Spain and for Central Europe (Heinemann et al., 2006; Lorenz et al., 2009a and b). The WRF model is state-of-the art in a massively parallel computing environment. The model offers numerous physical options such as planetary boundary layer, land-surface model, radiation, microphysics and cumulus parameterization. Currently, the WRF v3.3 supports several parameterizaton schemes among the above categories. In the present study, YSU and MYJ are used for PBL. Monin Obukhov with CarlsonBoland and Monin Obukhov with Zilitinkevich were used for surface layer while NOAH is also used for the surface physics. The RRTMG, FLG and Goddard were used for SW radiation. Furthermore, RRTM, FLG and Goddard were used for LW radiation. In microphysics, WSM6, and The Thompson were used while in cumulus the only Kain-Fritsch was used. Furthermore, clouds and their accompanying weather patterns are among the most important atmospheric phenomena limiting solar radiation at the Earth's surface. Because, cloud cover is one of the major factors restricting the availability of solar radiation at the Earth's surface. Cloud cover and global solar radiation showed a nonlinear relationshipdue to its dynamic chaotic characteristics (Chiacchio and Vitolo, 2012; Paulescu and Badescu, 2011). Therefore, clouds are a source of uncertainty in the predictions of solar irradiance. In model simulations, it can be seen that solar radiation has a strong dependency on the amount of cloud cover.

In particular, solar radiation in the absence of clouds (or "clear sky" condition) is generally easier to simulate than in cloudy conditions, as a proper representation of clouds is problematic. Besides, aerosols are mainly generated at ground surface. Specifically SAE experiences dust transport from desert regions, in nearby and remote areas. The aerosol optical depth (AOD) is a measure of aerosols distributed within a column of air from the Earth's surface to the top of the atmosphere over a vertical column of unit cross section. However, we did not examine the impact of aerosol on solar radiation here.

The aim of the present work is to forecast of hourly global horizontal irradiation (GHI) of the next 72 hours by using Weather Research Forecasting (WRF) model and to analyze the effect of parameterization on model performance for the two different periods including clear sky and cloudy conditions. Particularly, GHI forecast evaluation was carried out for the periods of August 20-23, 2011 for clear sky conditions and May 8-11, 2011 for cloudy conditions.

The study is carried out in both Marmara and Southeastern Anatolia (SEA) regions of Turkey. 72 hours model predictions were compared to ground based measurements at five sites in SEA and two sites in Marmara that were obtained from the archive of the Turkish State Meteorological Service. The evaluations were carried out for different forecast horizons (1, 2 and 3 days) for the two different cases (May and August).

2. Study Area and Data

Turkey is situated in Anatolia and the Balkans. The country has a total surface area of 783.562 km2. It is divided into seven geographic regions: In this study we considered Marmara and Southeastern Anatolia having the two contrast regions with regard to solar irradiance of Turkey. South Eastern Anatolia located in between latitudes 36–38 °N (see Fig. 1-a), covering a total area of about 75.000 km2 (7.5 million hectares), approximately 9.6% of the whole country. Marmara region is situated at northwest of Turkey (see Fig. 1-a). Its covering area is about 67.000 km2.

The SEA region has a border line with Syria and Iraq in the south and presents a varied topography. Particularly the southern part of the region is almost homogeneous flat area with a mean elevation of around 744 m asl. This area extends around the lower Tigris river basin, which flows into the Persian Gulf throughout the Mesopotamian plain. Furthermore, eastern part of the region presents a very complex topography, with steep elevation gradients reaching altitudes over 3800m asl. Cilo Mountain is the highest summit in the whole SEA.

The region is adjacent to the Eastern Anatolia to the north and the Mediterranean region on the west. The region has a semi-arid climate. The long summers are hot and dry in the region while the winters are cold with rainfall or snowfall. Neverthless, the topographic and geographic characteristics in this part of the region of Anatolia produce a wide range of weather and climate conditions. Particularly, one of the rainiest areas in the Anatolia Peninsula is located with the unique desert area in SAE. Rainfall is almost zero during the summer months even in August. Annual rainfall varies in between 440-665 mm. Şanlıurfa province including Ceylanpınar and Bozova receive minimum rainfall in the region while Sırnak and Mardin have measured about 650 mm. Furthermore, a

Figure 1 Maps showing the a) locations of Marmara and SEA regions and b) the solar irradiance ground stations operated by the Turkish Meteorological Service

giant national project application namely the Southeastern Anatolia Project (GAP) as dam lakes within the scope of the irrigation and with 17 hydroelectric power plants providing 8900 GWh is established since 1980s in the region. The total dam lake area is about 17,000 km2. Due to its impact on the local climate, rainfall has increased in the area. There are also two rivers (Tigris and Euphrates) were born here.

Marmara Region has a border with Greece and Bulgaria to the northwest. The average elevation of the region is around 101 m asl. Sea of Marmara connects to the Black Sea and the Aegean Sea, separating Turkey's European and Asian sides. The Marmara region has a Mediterranean climate and humid subtropical climate on the Aegean Sea coast and the south Marmara Sea coast. Moreover, there is an oceanic climate on the Black Sea coast and a humid continental climate in the interior. In summer, Marmara Region is warm to hot, humid and moderately dry whereas winters are cold and wet and sometimes snowy.

Global solar irradiation data are collected from 5 stations in SEA region and two stations in Marmara region. Figure 1-b and Table 1 show the locations of the solar irradiance ground stations operated by the Turkish Meteorological Service, in which GHI data are collected by Kipp & Zonen type pyranometers and standard quality control tests are applied by the State Meteorological Service, regularly.

Table 1 Location of the ground stations for Marmara and SEA regions

Region	Station name	Lat (º N)	Long (º E)	Alt (m)
MARMARA	Kırklareli	41.73	27.21	232
	Tekirdağ	40.95	27.49	4
SOUTHEASTERN ANATOLIA	Kilis	36. 71	37.11	640
	Ceylanpınar	36. 84	40.03	360
	Bozova	37. 37	38.51	622
	Şırnak	37. 52	42.45	1350
	Mardin	37. 31	40.73	1040

These stations were selected for their representative locations. For example Ceylanpınar is situated at the Şanlıurfa city which presents a semi-arid continental climate with Mediterranean influence. Annual average precipitation is about 439 mm in the region. The other stations in the region are Sırnak, Mardin, Kilis and Bozova. Bozova of Şanlıurfa is nearby (24 km) of the Ataturk dam in the region which is the largest dam in Turkey with a total surface area of 817.00 km^2. Mardin is one of the oldest settled areas in upper Mesopotamia which is the historical name of the region. The stations in the study have a measure sunshine duration in the range of 2852-3008 hr. Table 2 shows the characteristics of the cloudiness conditions of the sites for both periods that are defined according to ratio of sunshine duration.

Table 2 Characteristics of the cloudiness conditions of the sites for both periods

Region	Station name	8.05.2011	9.05.2011	10.05.2011	11.05.2011	20-23 August
Marmara	Kırklareli	Overcast	Broken	Broken	Broken	Clear
	Tekirdağ	Broken	Overcast	Broken	Broken	
Southeastern Anatolia	Kilis	Clear	Clear	Broken	Clear	
	Ceylanpınar	Clear	Clear	Broken	Clear	
	Bozova	Clear	Clear	Broken	Broken	
	Şırnak	Broken	Clear	Broken	Clear	
	Mardin	Clear	Clear	Clear	Broken	

(Clear: $S/S_0 > 0,75$, Broken: $S/S_0 < 0,25$, Overcast: $0,5 < S/S_0 < 0,75$)

3. WRF Model

Numerical weather prediction models have been proved to be powerful tools for short term solar radiation forecasting. In this study, global radiation is forecasted on an hourly basis using WRF numerical weather prediction model and compared to real measurements to validate the prediction. The simulations were driven based on the NCEP GFS data. The temporal resolution of the GFS analysis was 6h, while the spatial resolution was 1º.

The model domain's configuration is represented in Figure 2. The nested domains with decreasing horizontal resolutions of 36, 12 and 4 km are used for the outermost to innermost domains at Marmara and SEA regions.

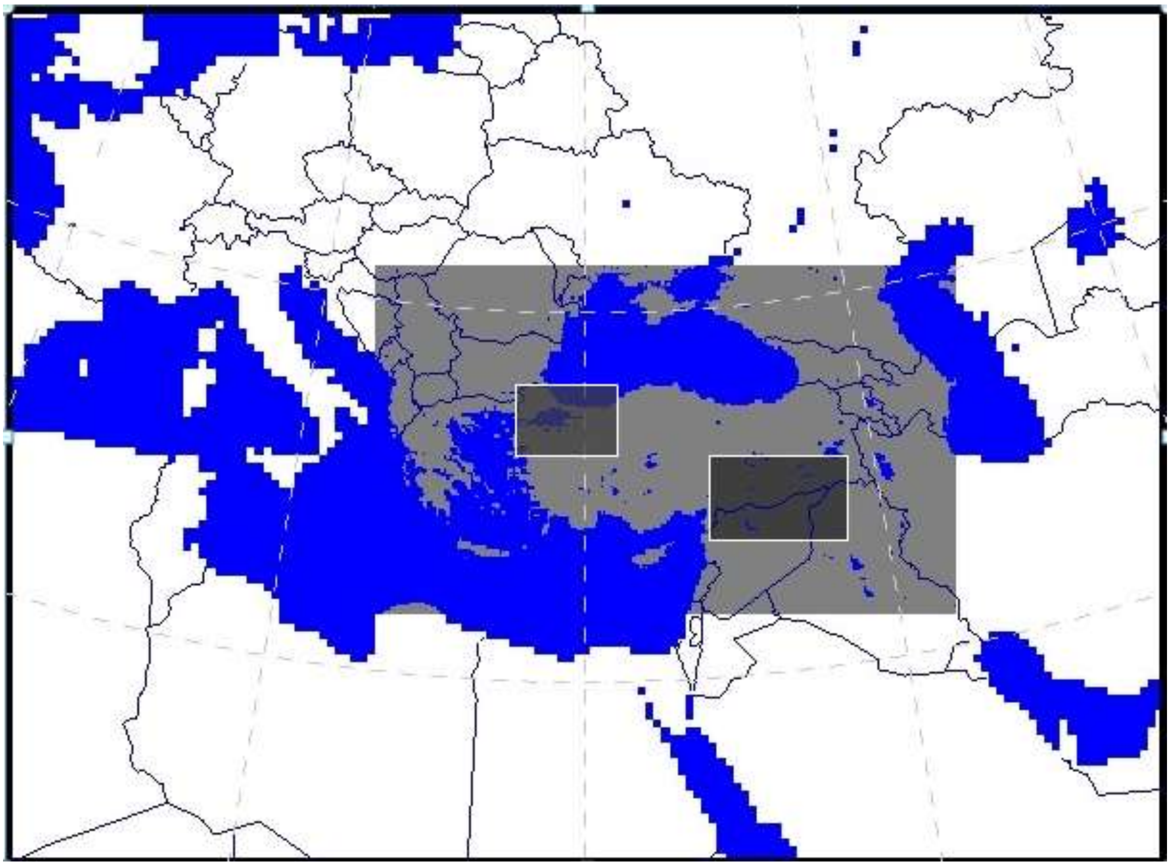

Figure 2 The WRF domains of the study regions.

The atmospheric column is decomposed into 35 vertical levels. The innermost domain was used in the evaluation procedure (Table 3). WRF (ARW, version 3) run for 72 hours for each case. 72 h GHI forecasts were evaluated based on hourly values measured in August 20-23, 2011 for clear sky days and in May 8-11, 2011 for cloudy days at the five sites in SAE region and two sites in Marmara region. Between domains 1 and 2, 2 and 3; and 2 and 4, the two way nesting option was selected. Model configurations are given in Table 3.

The WRF model has a wide range of physical parameterization. Physical processes that cannot be directly solved in model space require parameterization schemes. Several physics components have been included in WRF such as short wave and long wave radiation, microphysics, planetary boundary layer, and land-surface parameterizations.

Table 3 Model configuration

	Domain 1	**Domain 2**	**Domain 3 (Marmara)**	**Domain 4 (SEA)**
Horizontal grid intervals	36 km	12 km	4 km	4 km
Number of horizontal grids	146x108	220x133	130x106	157x97
Vertical Levels	35	35	35	35
IC/BC	GFS 1.0, 6hr intervals	Domain 1	Domain 2	Domain 2
Nesting	Two-way	Two-way	Two-way	Two-way
Cumulus	Kain Fritsch	Kain Fritsch	-	-

In this study, five different parameterization group defined from WFR0 up to WRF4 were used to evaluate the performance of the model. The physical parameterizations used in the study are presented in Table 4. RRTMG, RRTM, FLG, and Goddard radiation parameterizations were used for SW and LW with different microphysics groups in five configurations. The WSM6, the Thompson and Goddard were used for microphysics. Tested surface layer parameterizations were M-O with Carlson Boland and M-O with Zilitinkevich. NOAH used as surface physics, YSU and MYJ as PBL and Kain Fritsch as cumulus parameterizations.

Table 4 Parameterizations packages used in this study (WRF0 to WRF4)

Physical Schemes	**WRF0**	**WRF1**	**WRF2**	**WRF3**	**WRF4**
SW Radiation	RRTMG	RRTMG	FLG	Goddard	RRTMG
LW Radiation	RRTM	RRTM	FLG	Goddard	RRTM
Microphysics	WSM6	Thompson	Thompson	Goddard	WSM6
Surface Layer	Monin Obukhov with CarlsonBoland	Monin Obukhov with CarlsonBoland	Monin Obukhov with CarlsonBoland	Monin Obukhov with CarlsonBoland	Monin Obukhov with Zilitinkevich
Surface Phys.	NOAH	NOAH	NOAH	NOAH	NOAH
PBL	Yonsei Uni	Yonsei Uni	Yonsei Uni	Yonsei Uni	MYJ
Cumulus	Kain Fritsch	Kain Fritsch	Kain Fritsch	Kain Fritsch	Kain Fritsch

In radiation schemes, RRTMG_LW is a radiative transfer model that utilizes the correlated-k approach to calculate longwave fluxes and heating rates efficiently and accurately for application to GCMs (Mlawer et al., 1997). The RRTM LW radiation scheme uses Monte Carlo Independent Column Approximation (MCICA) method of random cloud overlap – statistical method to resolve sub-grid scale cloud variability. Finer resolution runs usually associated with WRF model means that clouds will most likely take up the entire grid space, in which case MCICA will not work. The Fu-Liou-Gu (FLG) radiation scheme (Gu et al., 2010; Gu et al., 2011) implemented in the WRF is based on the Fu-Liou scheme (Fu and Liou, 1992, 1993). The scheme uses a combination of the □-4-stream approximation for the solar flux (Liou et al. 1988) and the 2/4-stream approximation for the infrared flux to achieve a balance between accuracy and computational efficiency (Fu et al. 1997).

Goddard radiation package (original name CLIRAD) has been developed for two decades at NASA Goddard by Ming-Dah Chou and Max J. Suarez for use in general circulation models (GEOS GCM), regional model (MM5) and cloud-resolving models (GCE). The package is now included in NCAR WRF-ARW v3.3 released in spring 2011. Goddard radiative transfer modules can allow explicit interactions with microphysical processes (cloud optical property) -required for high-resolution WRF simulations (Chou and Suarez, 2001). Besides, Goddard radiative transfer modules can include aerosol direct effect by coupling the Goddard global aerosol transport model (i.e., GOCART aerosol mass and optical properties. Goddard shortwave scheme utilizes aerosol optical properties at 11 wavelengths, but they are zero in default WRF.

Michael J. Iacono and Thomas R. Nehrkorn Iacono and Nehrkorn showed that at the peak of each diurnal cycle, the Goddard SW model produces downward shortwave surface fluxes that are about 30 Wm-2 higher than RRTMG_SW, while the Dudhia SW flux as about 5 Wm-2 higher than RRTMG_SW.

In microphysics schemes, the WSM6 scheme has been one of the options of microphysical processes in the WRF model since 2004. The WSMP6 microphysics scheme is based on the revised ice-microphysics suggested by HDC (Hong and Jade Lim, 2006). In addition to the above characteristics, the WSM6 scheme behaves realistically in response to the appropriate grid resolvable forcing (Hong and Lim, 2006). For this purpose, we selected WSM6 for the 4 km resolution domains in the study. The Thompson is another scheme used for parameterization of microphysics developed for use in WRF and other mesoscale models. The Thompson microphysics parameterization scheme includes improvements to the earlier bulk scheme of Reisner (1998). It has been tested and compared with idealistic case studies specifically for midlatitudes (Hal et al., 2005). As compared to the previous microphysics scheme of physical process as well as software development the new parameterization incorporates a large number of terms. This scheme uses the latest scientific developments regarding ice nucleation, and includes a new dependence on aerosol concentration (Skamarock vd, 2008). Besides, the scheme includes the parameterization for calculating the direct radiative effects of several types of aerosol, including maritime, continental, urban, mineral dust, soot (black carbon), sea salt, and mineral dust. The radiative properties of aerosols, including the extinction coefficient, single-scattering albedo and asymmetry factor, are determined by their composition, shape and size distribution and are parameterized using the Optical Properties of Aerosols and Clouds (OPAC) database (Almeida et al. 1991; Tegen and Fung 1995; Tegen and Lacis 1996; Hess et al. 1998).

4. Results and Discussion

4.1. Case 1 (August 20-23, 2011-Clear Sky)

Figure 3 and 4 indicate that the modeled GHI is in close agreement with the observations for all seven sites for clear sky conditions in the August 2011 case study especially for Marmara region. Forecasts were evaluated in terms of the mean bias error (MBE) and the root mean square error (RMSE). RMSE that accounts for the spread of the error distribution and the lower the RMSE, the more accurate is the forecast. As seen in Figure 3, the forecast at Bozova and Kilis show clearly the highest and Şırnak the smallest uncertainties and forecast are obviously much more successful in Marmara region. Table 5 shows RMSE and MBE (W/m^2) of each site with each model parameterization package for August 2011 case for both regions. The MBE for clear sky conditions varies from site to site for each model configuration with a range from 8.87 W/m^2 (WRF2) to 55.76 W/m^2 (WRF3). Performance difference of WRF3, from the others is very clear. Relative RMSE and MBE values are also given in table 6 for each site. Regional average RMSE and MBE statistic can be seen in table 7. Minimum average MBE value is 0.136 with WRF2 package and minimum average RMSE value is 0.266 with WRF1 for SEA region. Average values reveal the ineffectiveness of WRF3 package.

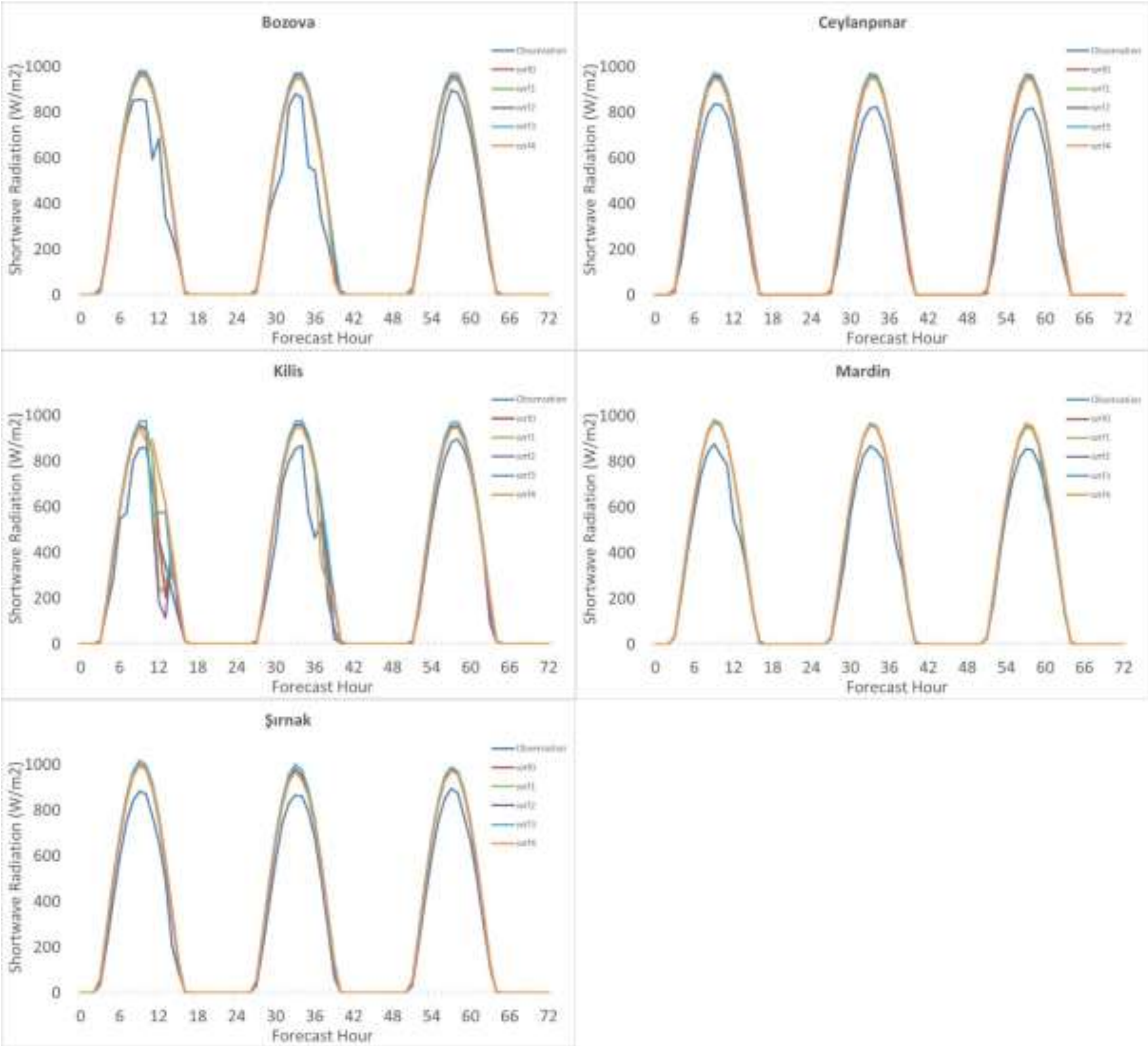

Figure 3 72 hours model predictions of GHI for clear sky conditions (20 August 2011 00z- 23 August 2011 00z, Bozova, Ceylanpınar, Kilis, Mardin and Şırnak)

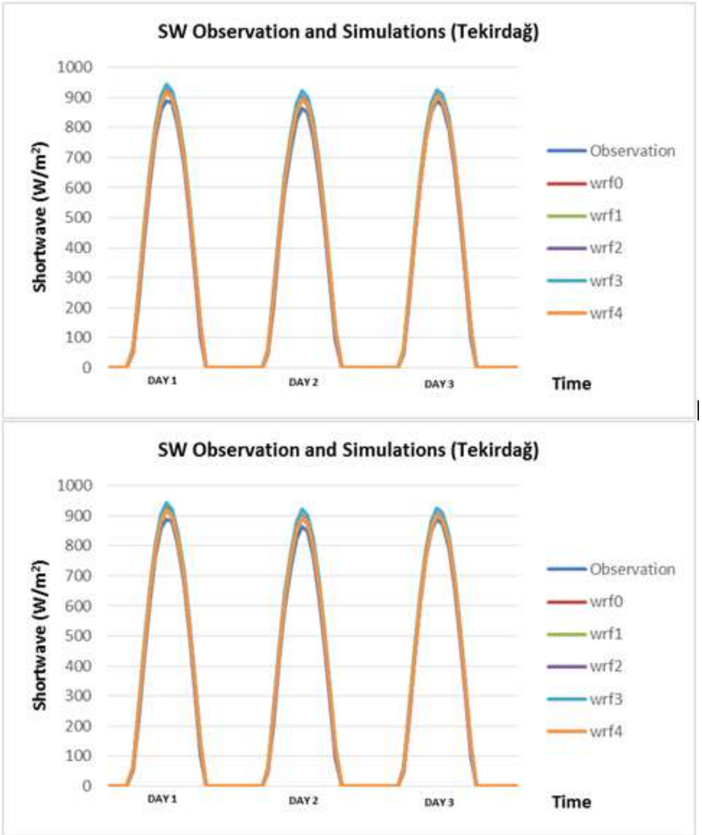

Figure 4 72 hours model predictions of GHI for clear sky conditions (20 August2011 00z- 23 August 2011 00z Kırklareli, Tekirdağ)

Table 5 RMSE and MBE iv W/m2 n for each site and for each model parameterization pacage for August 2011 case (both regions).

Site	Measure vs Model	WRF 0	WRF 1	WRF 2	WRF 3	WRF 4
Bozova	MBE	45.03	45.90	45.27	55.76	43.54
	RMSE	90.81	91.43	92.65	102.72	89.65
Ceylanpınar	MBE	46.97	46.28	44.86	55.32	47.34
	RMSE	71.75	69.10	69.23	82.04	70.66
Kilis	MBE	40.97	33.69	26.09	50.83	44.33
	RMSE	81.70	79.77	87.41	93.37	91.77
Mardin	MBE	34.68	34.72	31.47	31.47	37.18
	RMSE	57.71	57.63	57.43	57.43	60.10
Şırnak	MBE	39.89	39.54	35.98	47.94	38.32
	RMSE	58.69	58.26	55.42	70.11	56.65
Kırklareli	MBE	19.54	19.59	17.49	29.10	18.07
	RMSE	30.65	30.68	30.31	43.60	29.20
Tekirdağ	MBE	11.89	12.07	8.97	21.35	12.32
	RMSE	17.81	18.07	14.93	30.51	18.42

Table 6 The relative RMSE and MBE for each site and for each model parameterization package for August 2011 case for both regions.

Site	Measure vs Model	WRF 0	WRF 1	WRF 2	WRF 3	WRF 4
Bozova	rMBE	0,17	0,17	0,17	0,21	0,16
	rRMSE	0,34	0,34	0,35	0,39	0,34
Ceylanpınar	rMBE	0,18	0,18	0,17	0,21	0,18
	rRMSE	0,27	0,26	0,26	0,31	0,27
Kilis	rMBE	0,16	0,13	0,10	0,20	0,17
	rRMSE	0,32	0,31	0,34	0,36	0,35
Mardin	rMBE	0,12	0,12	0,11	0,11	0,13
	rRMSE	0,21	0,21	0,21	0,21	0,22
Şırnak	rMBE	0,14	0,14	0,13	0,17	0,14
	rRMSE	0,21	0,21	0,20	0,25	0,20
Kırklareli	rMBE	0.07	0.07	0.06	0.10	0.06
	rRMSE	0.11	0.11	0.11	0.16	0.10
Tekirdağ	rMBE	0.04	0.04	0.03	0.07	0.04
	rRMSE	0.06	0.06	0.05	0.11	0.06

Table 7 The average relative MBE and RMSE of the five different model configurations for the clear sky conditions in SEA Region.

	WRF 0	WRF 1	WRF 2	WRF 3	WRF 4
rMBE	0.154	0.148	0.136	0.180	0.156
rRMSE	0.270	0.266	0.272	0.304	0.276

4.2. Case 2 (May 8-11, 2011- Partly Coludy)

Figure 5-6 shows the simulations of GHI for cloudy days in May 2011 for the stations from SEA and Marmara regions. The simulations of the cloudy conditions clearly present the impact of parameterizations on the GHI forecasts. In these predictions, diurnal variation of the irradiance has been successfully captured, while significant differences are happened during the day. Both MBE and RMSE values are high values for cloudy conditions in May than its clear sky conditions in August. Table 8 shows RMSE and MBE of each site with each model parameterization package for the May 2011 case. The MBE for partly cloudy conditions varies from site to site for each model configuration with a range from 8.97 W/m^2 (WRF2) to 80.98 W/m^2 (WRF3) the same with clear sky conditions.

Table 9 presents normalized MBE and RMSE values for each parameterization sets. As seen in Table 9, the mean bias is always positive and vary in the range of 4-21%.

The regional averages statistics of each parametrizaton package are given in table 10 for SEA region. The lowest mean bias is found for WRF2 model configuration with 0.2 while the highest for WRF3 with 0.256. Furthermore, the best model configuration for the root mean square values are found for WRF0 with 0.538.

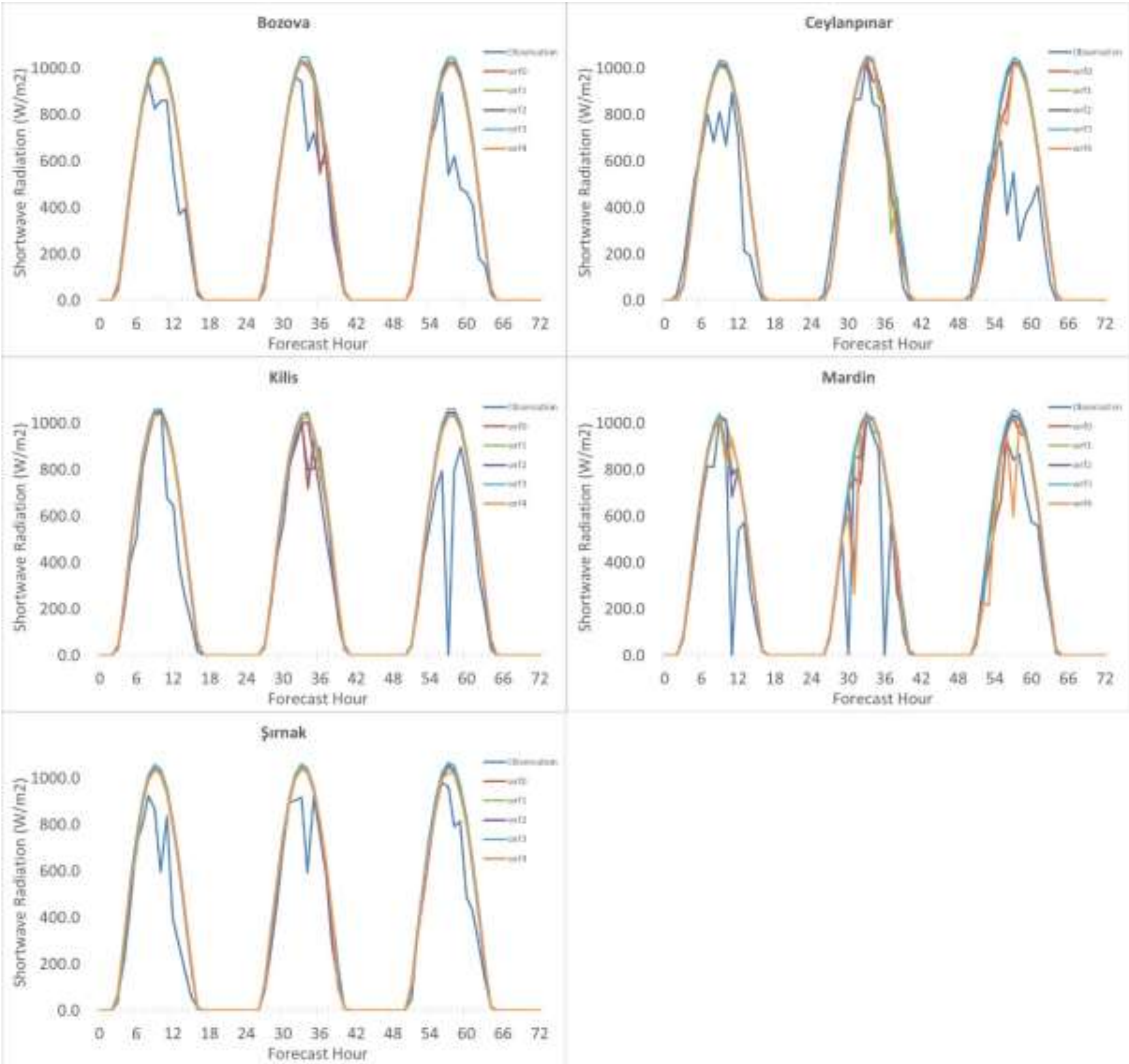

Fig.5. GHI forecasts and measurements for cloudy conditions (May 2011)

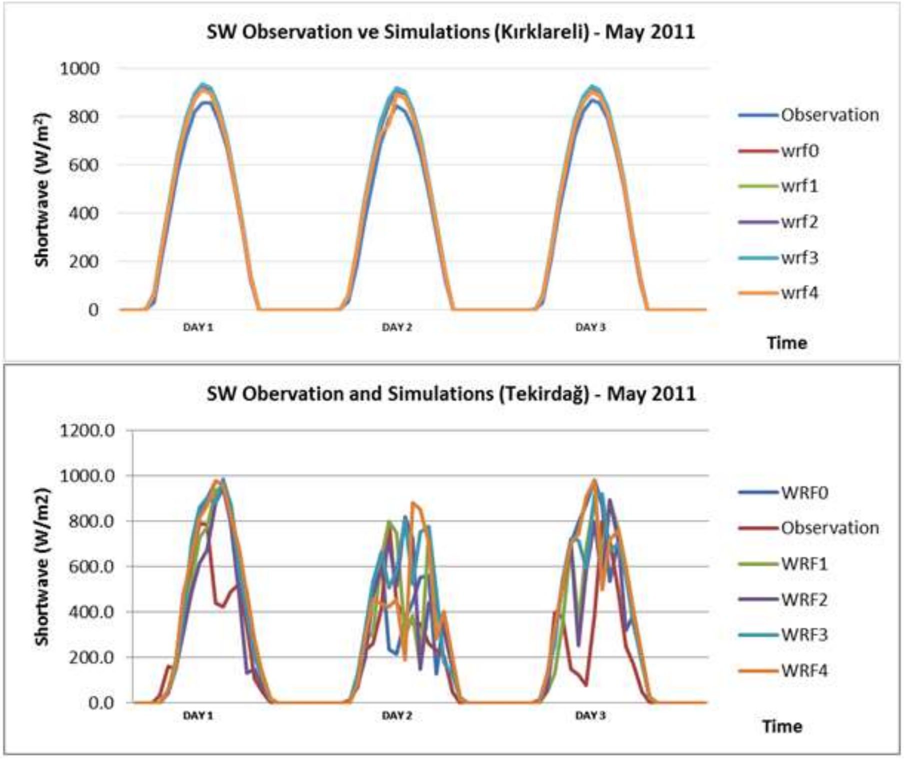

Fig.6. GHI forecasts and measurements for cloudy conditions (May 2011) - Marmara Region

Table 8 Results of statistical measures in W/m2 for cloudy conditions in site basis for the five model configurations - May 2011 (both region)

Site/station	Parameter	WRF 0	WRF 1	WRF 2	WRF 3	WRF 4
Bozova	MBE	62.06	64.58	58.88	73.89	63.58
	RMSE	139.49	141.54	139.94	151.40	139.63
Ceylanpınar	MBE	63.76	68.40	67.88	80.98	61.70
	RMSE	177.23	183.16	183.30	191.17	172.27
Kilis	MBE	56.70	58.64	49.49	68.57	61.41
	RMSE	148.89	151.44	152.44	159.48	151.26
Mardin	MBE	53.61	63.12	53.11	70.13	43.25
	RMSE	173.52	179.68	174.35	175.98	193.19
Şırnak	MBE	61.09	59.72	54.24	68.63	57.98
	RMSE	122.32	121.87	121.07	131.07	121.81
Kırklareli	MBE	19.54	19.59	17.49	29.10	18.07
	RMSE	30.65	30.68	30.31	43.60	29.20
Tekirdağ	MBE	11.89	12.07	8.97	21.35	12.32
	RMSE	17.81	18.07	14.93	30.51	18.42

Table 9 Verification results of cloudy conditions for each site and for the five model configurations - May 2011 (both region)

Site/station	Parameter	WRF 0	WRF 1	WRF 2	WRF 3	WRF 4
Bozova	rMBE	0,22	0,23	0,21	0,26	0,22
	rRMSE	0,49	0,50	0,49	0,53	0,49
Ceylanpınar	rMBE	0,23	0,25	0,25	0,30	0,23
	rRMSE	0,65	0,67	0,67	0,70	0,63
Kilis	rMBE	0,19	0,20	0,17	0,24	0,21
	rRMSE	0,51	0,52	0,52	0,55	0,52
Mardin	rMBE	0,19	0,23	0,19	0,25	0,15
	rRMSE	0,62	0,64	0,62	0,63	0,69
Şırnak	rMBE	0,21	0,20	0,18	0,23	0,20
	rRMSE	0,42	0,41	0,41	0,45	0,41
Kırklareli	rMBE	0.28	0.40	0.31	0.37	0.45
	rRMSE	0.96	0.89	0.77	0.89	1.08
Tekirdağ	rMBE	0.47	0.41	0.31	0.55	0.53
	rRMSE	1.20	1.03	0.95	1.13	1.26

Table 10 The average relative MBE and RMSE of the five different model configurations for the cloudy conditions (SEA Region.)

Parameter	WRF 0	WRF 1	WRF 2	WRF 3	WRF 4
rMBE	0.208	0.222	0.200	0.256	0.202
rRMSE	0.538	0.548	0.542	0.572	0.548

4.1. Site Based Findings

Average MBE and relative MBE statistic of each site for both clear sky and partly cloudy conditions are presented in table 11. MBE is positive for both two cases which indicates overestimation. Average relative RMSE and MBE statistics are also shown in table 12. As seen in table the normalized RMSE for cloudy conditions (May case) varies strongly from site to site. Furthermore, the forecasts at Ceylanpınar and Mardin show highest uncertainties while smallest at Şırnak. Besides, Sırnak site has the lowest RMSE for both August and May cases. But both Sırnak and Mardin site presents the lowest BIAS. However, the higher RMSE and higher BIAS are seen in Ceylanpınar and Bozova. Normalized bias is founded always positive in the range of 7-23%. Forecast validations show that error statistic of Marmara region distinctly lower than SEA region. This may be attributed to the aerosol characteristics of SEA region. In this region, dust storms are frequent, specifically in Mardin and surrounding areas. Mardin is known as the "dust city".

Table 11 Average relative MBE and MBE for the 72 hrs forecast at seven sites in both regions.

Site	Measure/Model Configuration	Clear sky (August)	Cloudy (May)
Bozova	MBE	47.10	64.60
	rMBE	0.18	0.23
Ceylanpınar	MBE	48.15	68.55
	rMBE	0.19	0.25
Kilis	MBE	39.18	58.96
	rMBE	0.15	0.22
Mardin	MBE	33.91	56.65
	rMBE	0.12	0.20
Şırnak	MBE	40.33	64.60
	rMBE	0.15	0.20
Kırklareli	MBE	20.76	72.08
	rMBE	0.07	0.36
Tekirdağ	MBE	13.32	83.57
	rMBE	0.05	0.45

Table 12 Average relative RMSE and RMSE (W/m2) for the72 hrs forecast at seven sites inboth regions

Site	Measure/Model Configuration	Clear sky (August)	Cloudy (May)
Bozova	RMSE	93.45	142.40
	rRMSE	0.35	0.50
Ceylanpınar	RMSE	72.55	181.43
	rRMSE	0.27	0.65
Kilis	RMSE	86.80	152.70
	rRMSE	0.34	0.52
Mardin	RMSE	58.06	179.34
	rRMSE	0.21	0.60
Şırnak	RMSE	59.83	123.63
	rRMSE	0.20	0.43
Kırklareli	RMSE	32.89	182.70
	rRMSE	0.12	0.92
Tekirdağ	RMSE	19.95	205.10
	rRMSE	0.07	1.12

Tekirdağ site has lowest RMSE for August case. There is no significant difference between Kırklareli and Tekirdağ in terms of bias values. The large errors of GHI are clearly seen for cloudy conditions in May case. The mean bias error values of GHI range from -25 to 101 W/m^2 in May (cloudy conditions) while from 11 to 57 W/m2 in August (clear sky conditions). RMSE values for cloudy conditions in May range in 121 – 193 W/m^2 while for clear sky conditions in August ranging with 55 to 102 W/m2. The cloud influences enhance this result.

5. Conclusions

The performance of the GHI forecasting based on the WRF mesoscale model including five different parameterization schemes for radiation, microphysics, planetary boundary layer and cumulus were analyzed based on hourly values of solar irradiation measured in May 8-11, 2011 representing cloudy conditions and August 20-23, 2011 for clear sky conditions.

The results are followed:

- The WRF Model tends to overestimate the GHI for all sites. MBE is found positive in all cases. This may be attributed to the default tuning of the WRF solar irradiance scheme accounts for ozone absorbtion and aerosol attenuation to gether.
- RMSE which accounting for the spread of the error distribution decreases under clear sky conditions.
- Both MBE and RMSE values are high values for cloudy conditions in May case than its clear sky conditions in August case.
- In both cloudy and clear sky conditions, the averaged normalized RMSE values present similar result except WRF3. The result of the WRF0 scheme is slightly better than the others for cloudy conditions. The result of the WRF1 scheme is much better than the other schemes for clear sky conditions. The only difference between the WRF0 and WRF1 schemes is the microphysics. WRF0 uses WSM6 while WRF1 uses the Thompson schemes.
- In cloudy conditions, the averaged normalized RMSE values are similar except WRF3, which includes Goddard scheme. It is clearly seen that Goddard Scheme present the poor results in both cloudy and clear sky conditions compared to the other schemes.
- The better performance of the model has been found in Marmara region.
- Clouds are a source of certainty. Therefore extensively ground–based cloud measurements are needed.
- As a future study, the cloud and dust sensitivity analysis should be perform

Acknowledgements

This study has been a part of the Project 111Y234 supported by TUBITAK (Turkish Scientific and Technological Research Council). The authors would like to thank TSMS for the data support.

REFERENCES

Alta D., C.ertekin, F.Evrendilek, 2010, Quantifying spatio-temporal dynamics of solar radiation exergy over Turkey, Renewable Energy, 35, 2821-2828.

Badarinath, K.V.S., S. K. Kharol, D.G. Kaskaoutis, H.D. Kambezidis, (2007): Influence of atmospheric aerosols on solar spectral irradiance in an urban area. Journal of Atmospheric and Solar-Terrestrial Physics. 69, 589-599.

Bakırcı.K, Correlations for estimation of daily global solar radiation with hours of bright sunshine in Turkey, Energy, 2009, 39,485-501.

Bo H., W. Yuesi, L. Guangren, (2010): Properties of ultraviolet radiation and the relationship between ultraviolet radiation and aerosol optical depth in China. Atmospheric Research 98, 297-308.

Bulut.H,and O.Büyükalaca, 2007, Simple model for the generation of daily global solar-radiation data in Turkey, Applied Energy, 84, 477-491.

Chiacchio and Vitolo, 2012, Effect of cloud cover and atmospheric circulation patterns on the observed surface solar radiation in Europe, JGR, 117, DOI: 10.1029/2012JD017620. published online: 22 SEP 2012.

Chou M.-D., and M. J. Suarez, 2001: A thermal infrared radiation parameterization for atmospheric studies. NASA/TM-2001-104606, vol. 19, 55pp

Dudhia J., 1989. Numerical study of convection observed during the winter monsoon experiment using a mesoscale two-dimensional model. J. Atmos. Sci. 46, 3077–3107.

EIEI, 2013 General directorate of electrical power resources survey and development administration. http://www.eie.gov.tr/eie-web/english/solar/solarTurkey_e.html

Falayi, E.O and Rabiu, A.B, 2011, Estimation of global solar radiation using cloud cover and surface temperature in some selected cities in Nigeria, Archives of Physics Research, 2011, 2, 99-109

Grell , G., Dudhia, J., Stauffer, D., 1998. A Description of the Fifth- Generation Penn State/NCAR Mesoscale Model (MM5). NCAR Tech. Note, NCAR/TN-398+STR, USA.

Gu, Y., Liou, K. N., Ou, S. C., and Fovell, R.: Cirrus cloud simulations using WRF with improved radiation parameterization and increased vertical resolution, J. Geophys. Res., 116, D06119, doi:10.1029/2010JD014574, 2011

Hall W.D. , R.M.Rasmussen, G.Thompson, 2005, The new Thompson microphysical scheme in WRF, WRF/MM5 user's workshop – June 2005.

Heinemann, D., Lorenz, E., Girodo, M., 2006. Forecasting of solar radiation. In: Dunlop, E.D., Wald, L., Sˇ u´ ri, M. (Eds.), Solar Energy Resource Management for Electricity Generation from Local Level to Global Scale. Nova Science Publishers, Hauppauge.

Goody, R., R. West, L. Chen, and D. Crisp, 1989: The correlated-k method for radiation calculations in nonhomogeneous atmospheres. Journal of Quantitative Spectroscopy and Radiative Transfer, 42, 539-550.

Hong, S.-Y., and J.-O. J. Lim, 2006, The WRF Single-Moment 6-Class Microphysics Scheme (WSM6), J. Korean Meteor. Soc., 42, 129–151.

IEA, 2013: PVPS Report, IEA-PVPS T1-22.

IPCC, 2011:In IPCC Special Report on Renewable Energy Soucess and Climate Change Mitigation.

Lara-Fanego, V., J. A. Ruiz-Arias, A. D. Pozo-Vázquez, C. A. Gueymard and J. Tovar-Pescador, Evaluation Of DNI Forecast Based On The WRF Mesoscale Atmospheric Model For CPV Applications,

CPV-8 Conference, Toledo, Spain, 2012.

Lara-Fanego, V., et al., 2011. Evaluation of the WRF model solar irradiance forecasts in Andalusia (southern Spain). Sol. Energy,doi:10.1016/j.solener.2011.02.014.

Lorenz. E., Remund, J., Mu¨ ller, S.C., Traunmu¨ ller, W., Steinmaurer, G., Pozo, D., Ruiz-Arias, J.A., Fanego, V.L., Ramirez, L., Romeo, M.G.,Kurz, C., Pomares, L.M., Guerrero, C.G., 2009a. Benchmarking of different approaches to forecast solar irradiance. In: 24th European Photovoltaic Solar Energy Conference, Hamburg, Germany, 21–25 September 2009.

Lorenz, E., et al., 2009. Irradiance forecasting for the power prediction of grid-connected photovoltaic systems.

IEEE J. Selected Topics Appl. Earth Observations Remote Sens. 2 (1).

Kharol S.K., K.V.S. Badarinath, A.R. Sharma, D.G. Kaskaoutis, H.D. Kambezidis, (2011): Multiyear analysis of Terra/Aqua MODIS aerosol optical depth and ground observations over tropical urban region of Hyderabad, India. Atmospheric Environment, 45, 1532-1542.

Mlawer, E. J., S. J. Taubman, P. D. Brown, M. J. Iacono, and S. A. Clough, 1997: Radiative transfer for inhomogeneous atmosphere: RRTM, a validated correlated-k model for the longwave. J. Geophys. Res., 102 (D14), 16663–16682.

Ogunjobi, K.O., Y.J. Kim, (2004): Ultraviolet (0.280–0.400 Am) and broadband solar hourly radiation at Kwangju, South Korea: analysis of their correlation with aerosol optical depth and clearness index. Atmospheric Research 71, 193-214.

Hideaki Ohtake a,⇑ , Ken-ichi Shimose a, Joao Gari da Silva Fonseca Jr.

Takumi Takashima, Takashi Oozeki, Yoshinori Yamada, 2012, Accuracy of the solar irradiance forecasts of the Japan Meteorological Agency mesoscale model for the Kanto region, Japan, Solar Energy, xxx–xxx.

Morcrette, J., Bechtold, P., Beljaars, A., Benedetti, A., Bonet, A., Doblas- Reyes, F., Hague, J., Hamrud, M., Haseler, J., Kaiser, J., Leutbecher, M., Mozdzynski, G., Razinger, M., Salmond, D., Serrar, S., Suttie, M., Tompkins, A., Untch, A., Weisheimer, A., 2007. Recent advancesin radiation transfer

parameterizations. ECMWF Tech. Memo. 539, 1–52.

Ozer B, E.Gorgun, S.Incecik, 2013, The scenario analysis on CO2 emission mitigation potential in the Turkish electricity sector: 2006-2030, Energy, 40, 395-403.

Paulescu , M and Badescu, V., Theor Appl Climatology, 2011, 103:459–470.

Perez R., Kivalov, S., Schlemmer, J., Hemker Jr., K., Renne´, D., Hoff, T.,2009. Validation of short and medium term operational solar radiation forecasts in the US. In: Proceedings of the ASES Annual Conference,Buffalo, New York.

Perez,R, R. Seals, R. Stewart, A. Zelenka and V. Estrada-Cajigal, 1994, Using Satellite-Derived Insolation Data for the Site/Time Specific Simulation of Solar Energy Systems, Solar Energy, 53, 6; 7pp.

Remund , R., Perez, Lorenz, E., 2008. Comparison of solar radiation forecasts for the USA. In: Proceedings of the 23rd European Photovoltaic Solar Energy Conference, 2008, Valencia, Spain, pp. 1.9–4.9.

Skamarock, W.C., Klemp, J.B., Dudhia, J., Gill, D.O., Barker, D.M.,Duda, M.G., Huang, X.Y., Wang, W., Powers, J.G., 2008. A Description of the Advanced Research WRF Version 3, NCAR/TN-475+STR, Mesoscale and Microscale Meteorology Division, NationalCentre for Atmospheric Research, Boulder, USA.

Zamora, R.J., Dutton, E.G., Trainer, M., McKeen, S.A., Wilczak, J.M., Hou, Y.T., 2005. The accuracy of solar irradiance calculations used in mesoscale numerical weather prediction. Mon. Weather Rev. 133, 783–792.

Zamora, R.J., Solomon, S., Dutton, E.G., Bao, J.W., Trainer, M., Portmann, R.W., White, A.B., Nelson, D.W., McNider, R.T., 2003.Comparing MM5 radiative fluxes with observations gathered during the 1995 and 1999 Nashville southern oxidant studies. J. Geophys. Res. 108 (D2), 4050.